Rapid Stabilization of Immiscible Fluids using Nanostructured Interfaces via Surfactant Association

Zahra Niroobakhsh,[1] Jacob A. LaNasa,[2] Andrew Belmonte,[2,3] and Robert J. Hickey[2,4,*]
[1]Department of Civil and Mechanical Engineering, University of Missouri-Kansas City, Kansas City, Missouri 64110, USA
[2]Department of Materials Science & Engineering, Pennsylvania State University, University Park, Pennsylvania 16802, USA
[3]Department of Mathematics, Pennsylvania State University, University Park, Pennsylvania 16802, USA
[4]Materials Research Institute, Pennsylvania State University, University Park, Pennsylvania 16802, USA

(Received 14 October 2018; published 3 May 2019)

Surfactant molecules have been extensively used as emulsifying agents to stabilize immiscible fluids. Droplet stability has been shown to be increased when ordered nanoscale phases form at the interface of the two fluids due to surfactant association. Here, we report on using mixtures of a cationic surfactant and long chained alkenes with polar head groups [e.g., cetylpyridinium chloride (CPCl) and oleic acid] to create an ordered nanoscale lamellar morphology at aqueous-oil interfaces. The self-assembled nanostructure at the liquid-liquid interface was characterized using small-angle x-ray scattering, and the mechanical properties were measured using interfacial rheology. We hypothesize that the resulting lamellar morphology at the liquid-liquid interface is driven by the change in critical packing parameter when the CPCl molecules are diluted by the presence of the long chain alkenes with polar head groups, which leads to a spherical micelle-to-lamellar phase transition. The work presented here has larger implications for using nanostructured interfacial material to separate different fluids in flowing conditions for biosystems and in 3D printing technology.

DOI: 10.1103/PhysRevLett.122.178003

Amphiphilic systems using oil, water, and surfactants have been utilized in a variety of applications ranging from oil recovery and drug delivery, to food and personal care products [1–4]. The main objective of amphiphilic surfactant systems is to increase emulsion stability and control colloidal structures at the nanoscale [5,6]. Beyond emulsion stability and colloidal morphology control, mixtures containing immiscible fluids and surfactantlike molecules exhibit intricate phase diagrams containing various morphologies and phase behavior of different universality classes [7–10]. Furthermore, nontraditional amphiphiles can be used to impart responsive behavior in colloidal systems [11] and contribute to innovations in biomedical, energy, and separation technologies [12–21]. Since the pioneering work on surfactant association structures by Friberg and co-workers, extensive work has been conducted over the past 50 years in the area of nanostructured phases that form between two interfaces (fluid-fluid and fluid-gas) [22–27]. In most cases, the static structure was investigated, while little attention has been focused on the *in situ* structural self-assembly process of surfactant association at interfaces. This includes oppositely charged surfactant systems, also referred to as a catanionic system [28–32], which form double-chained surfactants that resemble zwitterionic amphiphiles and lead to stiff and ultrastable membranes [6,33–36]. Most cationic and anionic surfactants components are assembled in aqueous systems [28–31]. However, immiscible catanionic systems have recently attracted much attention where a hydrophobic fatty acid is used in place of anionic surfactants [33,37–44]. Unlike many immiscible multicomponent systems, fatty acid catanionic systems only require a combination of three components. Since fatty acids have dual properties as an oil phase and amphiphile, this could offer new possibilities in designing bulk proton conductors [40].

In general, studies on such systems have been mainly conducted under static conditions and at thermodynamic equilibrium. However, research on dynamic phenomena in which structural self-assembly stabilizes the interface under nonequilibrium conditions is still in its infancy. This is despite the fact that *in situ* self-association of amphiphilic molecules has been widely observed for a variety of practical or industrial applications including oil recovery [45–47], flow instabilities [20,48–51], biological systems [52–54], and rare metal extraction [55]. There has yet to be a fundamental study on dynamics of interfacial material formation between associating surfactants at immiscible liquid interfaces, and the connection between structure and property relationships, in addition to the underlying mechanism of structure development at the molecular level. Stabilizing immiscible fluid interfaces with associating surfactants that self-assemble rapidly and form elastic materials have many exciting applications such as separating fluids for encapsulation of desired cargo for drug delivery, or for printing three-dimensional structures to resemble biosystems such as veins and arteries.

Here, we show how immiscible mixtures containing a cationic surfactant [cetylpyridinium chloride (CPCl)] and a long chain alkene with a polar head [e.g., oleic acid (OA)] will stabilize aqueous-oil interfaces via a spherical micelle-to-lamellar phase transition. The lamellar phase creates an interfacial material that spontaneously forms when an aqueous solution of CPCl encounters OA. We hypothesize that the lamellar morphology that self-assembles at the aqueous-oil interface is driven by the change in critical packing parameter of the CPCl molecules that form the aqueous micellar solution. Amphiphiles that form micelles in water have a critical packing parameter, $v/a_0 l_c \leq \frac{1}{3}$, whereas lamellar structures have $v/a_0 l_c \approx 1$, where a_0, v, l_c are the surface area of the hydrophilic head group, the hydrocarbon chain volume, and critical length, respectively [6]. The change in $v/a_0 l_c$, favoring the lamellar morphology, when CPCl encounters OA is predicted to occur due to the dilution of the CPCl surfactant molecules via OA association, which minimizes the electrostatic interactions between pyridinium head groups. The system undergoes distinct flow instabilities from droplets to flowing columns by injecting a CPCl solution into an OA reservoir, where the interface is stabilized by a lamellar nanostructure. The formation of nanostructured interfacial materials exhibiting elastic mechanical properties will allow for the rapid printing of self-supporting structures.

Aqueous surfactant solutions containing spherical micelles have been previously shown to develop various interfacial instabilities when the micelles come into contact with a second solution such as NaSal solution or fatty acid [48–50]. Here, we show that similar interfacial instabilities form when a CPCl solution is injected into OA. By injecting CPCl solutions with varying concentrations into an OA reservoir at a fixed flow rate, different states can be made, as shown in Fig. 1. The description of the experimental setup has been previously published [48].

At 0 mM CPCl, surface-driven pinch-off is observed. At a surfactant concentration greater than the critical micelle concentration (CMC = 0.9 mM [56]), the droplets become smaller and deformed, while increasing in number, as shown in Fig. 1(b). Further increase of the CPCl concentration results in a transition from droplets to columnlike geometries. At 190 mM, the column surface is unstable and forms a wavylike shape [Fig. 1(c)], while at 425 mM the column has smooth surface and buckles [Fig. 1(d)]. The structural changes with respect to CPCl concentration as shown in Fig. 1 are hypothesized to be a result of an interfacial material that forms at higher CPCl concentrations. Therefore, we decided to investigate the interfacial material that forms at the liquid-liquid interface to understand why immiscible fluids are stabilized at increased CPCl concentrations. This enables the identification of mechanisms underlying the observed interfacial dynamics.

We used small-angle x-ray scattering (SAXS) to determine the morphology of the interfacial material. We were able to create and characterize interfacial materials by quickly adding OA to a CPCl solution while in a quartz capillary tube (see Supplemental Material [57]). On addition of the OA to the CPCl solution, a white interfacial material began to form instantly, which allowed for direct SAXS characterization of the material. The thickness of the interfacial material increases with time while in the capillary. The interfacial material thickness for 50 mM CPCl/OA is roughly 0.1 mm after 20 min, and increases to roughly 0.3 mm after 3 h (see Fig. S1 of the Supplemental Material [57]). Figure 2(a) shows the SAXS measurements for the oil phase, the aqueous phase, and the interfacial material at different time points for the 190 CPCl solution. The upper layer (OA phase) shows a typical scattering pattern for a fluid with no inherent nanostructure. For the CPCl solutions, the SAXS patterns exhibit a structure factor indicative of a disordered spheroidal micellar phase, which is similar to previously published works [58,59]. Even though the beam size (0.6×0.5 mm) is larger than the interfacial material thickness, the isotropic scattering shown in Fig. S2 of the Supplemental Material [57] indicates that there are no scattering artifacts as a result of the simultaneous illumination of the different liquid-film interfaces.

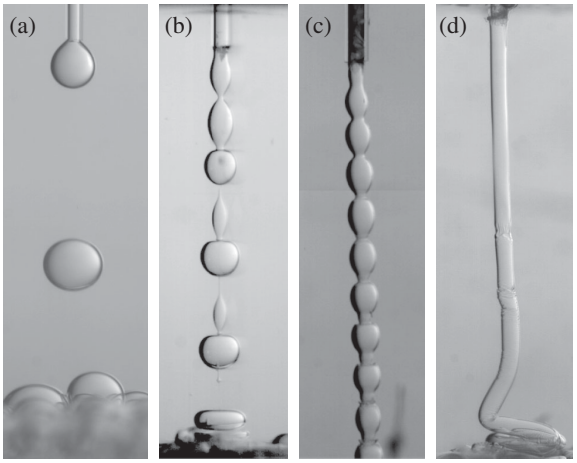

FIG. 1. Photographs showing the distinct structural changes when CPCl solutions of varying concentration are injected into an oleic acid reservoir at fixed CPCl injection rate of $Q = 100$ ml/h: (a) 0 mM CPCl, (b) 50 mM CPCl, (c) 190 mM CPCl, and (d) 425 mM CPCl.

The scattering patterns at the interfacial layer is drastically different from the OA and CPCl phases. The SAXS patterns suggest that the interfacial material possesses a lamellar nanostructure (LAM, $q/q^* = 1, 2$ where q^* is the first reflection). We hypothesize that the lamellar phase is comprised of CPCl/OA bilayers alternating between layers of water. The lamellar domain spacing (d) is calculated using $d = 2\pi/q^*$ which constitutes one layer of each water and CPCl/OA bilayer. For the 190 mM CPCl solution, the lamellar spacing is calculated to be 14.0 nm. The lamellar phase located between the CPCl and OA phases does not

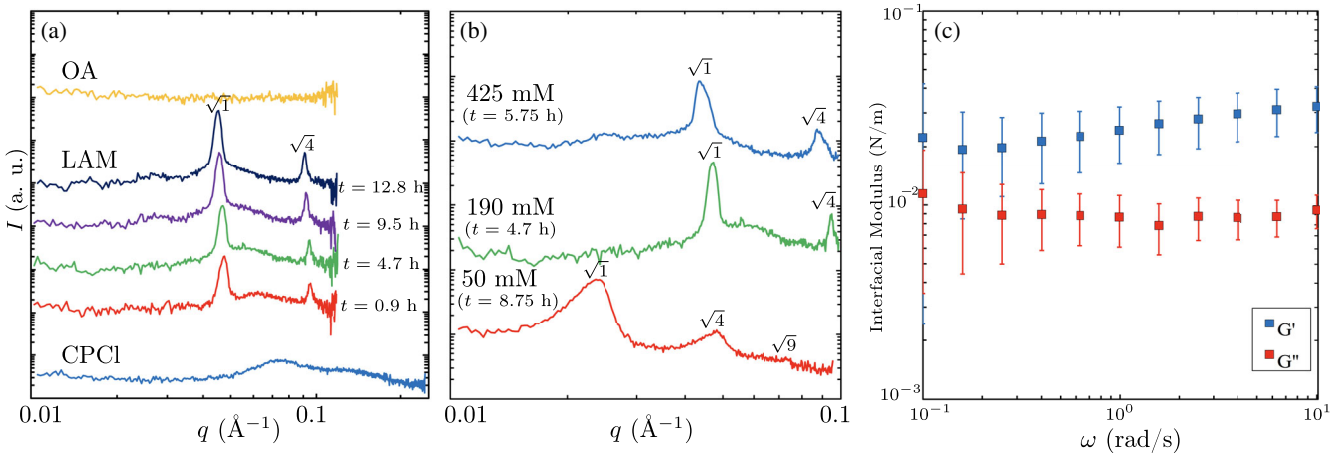

FIG. 2. (a) SAXS patterns showing the interfacial structure of the 190 mM CPCl solution and OA at different times (t) after contact. (b) SAXS patterns showing interfacial nanostructure formed with CPCl solutions of varying concentrations at extended times. (c) Averaged interfacial moduli of four frequency sweep measurements at fixed 0.1% strain and immediately after sample loading for 190 mM CPCl/OA.

change appreciably over time, as the primary scattering peak moves slightly to lower q. This is different from the overall thickness of the interfacial material discussed earlier. The lamellar morphology is observed at different CPCl concentrations, as shown in Fig. 2(b). The domain spacing initially decreases with increasing CPCl concentration (from $d \sim 26$ nm for 50 mM to $d \sim 14$ nm for 190 mM). Then the domain spacing stays relatively constant for the concentrations 190 and 425 mM. We posit that the decrease in the lamellar domain spacing with increasing CPCl concentration is due the greater availability of the CPCl molecules with respect to the water content. For example, the thickness of the hydrophobic domains is not expected to change with CPCl concentration, as the length of the hydrophobic chains dictate the hydrophobic domain thickness. Therefore, the decrease in the domain spacing is assumed to be a result of less water separating the hydrophobic layers.

Motivated by the structure of the interfacial material formed between the oil and aqueous phases, the mechanical response was characterized using interfacial rheology employing double-wall-ring geometry (DWR). Figure 2(c) shows the frequency sweep measurements at 0.1% strain and the fixed angular frequency of 5 rad/s (linear viscoelastic region) for 190 mM CPCl. There is a larger storage modulus G' than loss modulus G'', while both moduli remain insensitive to frequency. This reveals typical solidlike viscoelastic behavior for the interfacial material. Similar behavior is observed for 425 mM (see Supplemental Material [57], Fig. S4). We also observe an increase in moduli with increasing the CPCl solution concentration. However, the reason for the increase in the modulus with increasing CPCl concentration is not easily discernible as the interfacial material thickness increases over time. Previous experimental and modeling results indicate that catanionic bilayers exhibit increased bending moduli due to the electrostatic ordering of cations and anions in the membrane, which could potentially play a role in our system [34,60]. Further analysis is needed to fully determine if the increase in the modulus is indeed a result of CPCl concentration, which would effect the interfacial material thickness or molar ratio between CPCl and OA in the self-assembled bilayer.

We hypothesize that the continuous self-supporting tube is more uniform at increased CPCl concentrations [Fig. 1(d)] due to an increase in the mechanical properties of the interfacial layer. The claim is supported by both the SAXS and the interfacial rheology experiments. All three CPCl concentrations show that the interfacial layer exhibits a LAM morphology, while interfacial rheology experiments show that the 425 mM CPCl sample exhibits the largest modulus. Therefore, the LAM morphology contributes to the mechanical properties associated with the interfacial material, but there must be additional factors at play giving rise to the smooth self-supporting tube. The question to answer is then, "If the morphology of the interfacial material is not leading to a smoother column surface, then why would the mechanical properties be a factor, and why would the interfacial modulus increase with increasing CPCl concentration?" One possibility is that the lamellar phase forms more rapidly, and as a result, thickens at a greater rate at higher CPCl concentrations. This would occur because there are more micelles per volume at increased CPCl concentrations (see Supplemental Material [57]). The second possibility is that the CPCl/OA molar ratio in the bilayer membrane contributes to the bending rigidity. Modeling results indicate that the bending moduli of catanionic bilayers is sensitive to the molar ratio between cation and anion surfactants [34]. Here, proton nuclear magnetic resonance (^{1}H NMR) experiments confirm that there is an increase in the CPCl:OA ratio with

increasing CPCl concentration (see Supplemental Material [57]). We do not currently have experimental results to support one possibility over the other, but we are actively working in this area.

The SAXS results in Fig. 2 support our hypothesis that the lamellar morphology formation occurs via a micelle-to-lamellar transition due to the dilution of the cationic head groups of CPCl when they come in contact with OA. The work shown here follows an established model developed by Jonsson and Wennerstrom for water-soap-alcohol mixtures in which the alcohol acts as a cosurfactant [61]. The thermodynamic model by Jonsson and Wennerstrom incorporates the electrostatic contribution of the charged surfactant (e.g., CPCl) to the free energy and the chemical potentials, and shows how the addition of a cosurfactant dilutes the ionic surfactant, which increases the hydrocarbon volume and minimizes the free energy of the polar-apolar interface.

We would like to differentiate the system shown here from catanionic systems that form soft glassy materials at liquid-air interfaces [33]. In the previously reported system, catanionic vesicles dispersed in aqueous solution aggregate at the air-water interface over time yielding a solidlike lamellar interface. In our system, we have a morphology transition at the liquid-liquid interface that occurs within seconds, which is different from the phase transition of the catanionic vesicles at a liquid-air interface over the matter of weeks [33].

Here, we predict that there is a rapid micelle-to-lamellar morphology transition due to the presence of the OA cosurfactant, and over time, the thickness of the interfacial material grows due to the OA molecules diffusing into the CPCl micellar phase, and leading to the formation of a successive lamellar layer underneath as illustrated in Fig. 3(a). In Fig. 3(a), the lamellar structure is aligned parallel to the interface. However, it is likely that there are lamellar domains randomly oriented as the two-dimensional scattering pattern (Fig. S2 of the Supplemental Material [57]) is isotropic.

Although previous work suggests that the OA is ionized [37,42], which would lead to an electrostatic interaction between the cationic and anionic surfactants causing a change in the critical packing parameter, we predict that the self-assembly process in the work described here is due to the cosurfactant effect [62]. To test if the cosurfactant effect is indeed causing the micelle-to-lamellar morphology change, we used oleyl alcohol (OAL) and oleylamine (OAM) as the oil instead of OA. Both OAL and OAM are neutral and will not have electrostatic interactions between CPCl. When a solution of CPCl (100 mM) was added to either an oil reservoir of OAL or OAM, a similar interfacial material formed and resembled the same material when OA is used (see Fig. S1b of the Supplemental Material [57]). Interestingly, the interfacial material formed using OAL and OAM exhibited a lamellar

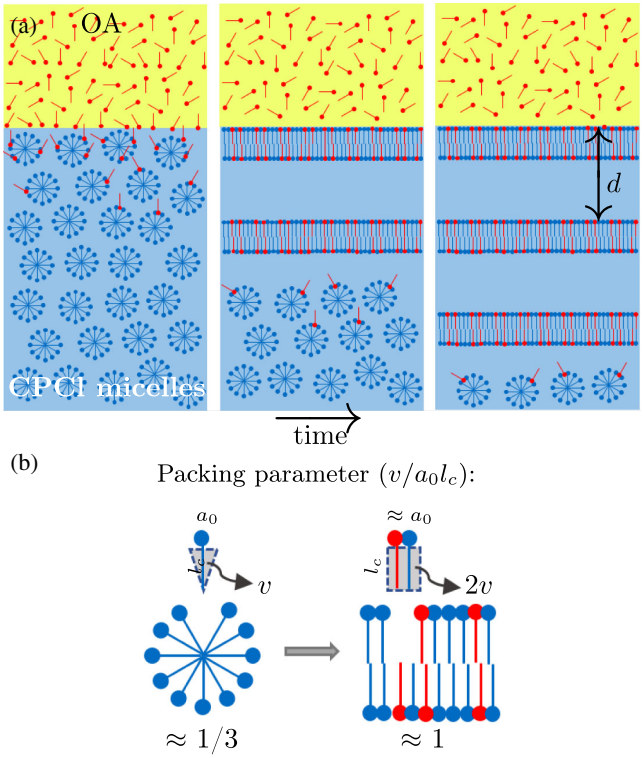

FIG. 3. (a) Schematic illustration of the possible interfacial material formation and the time evolution of the OA/CPCl solution interface; (b) the packing parameter estimation responsible for the structural transition.

morphology, as determined by indexing the SAXS pattern, for both OAL and OAM [Fig. 4(a)]. Therefore, we suggest that when the CPCl micelles interact with an oil that acts as a cosurfactant, we can stabilize liquid-liquid interfaces with ordered nanostructures.

By invoking the packing parameter argument, we suggest that the micelle-to-lamellar morphology transition is a result of an increase in $v/a_0 l_c$ from $\sim 1/3$ (micelle) to ~ 1 (bilayer) due to the dilution of the cationic head groups, as shown in Fig. 3(b). While we propose that the lamellar morphology should have a packing parameter of approximately 1, alternative mechanisms might involve the formation of vesicles first, and then the transition to lamellar structures. Additional work is needed to specifically determine the role the packing parameter plays in the morphology transition, and ways to control the final morphology.

We can take advantage of the rapid self-assembly behavior in our system to print liquid-in-liquid structures. For instance, Fig. 4(b) shows a manually printed spiral by injecting 425 mM CPCl into OA reservoir. This offers a novel method to print complex objects in liquid-liquid environments suitable for biomaterials such as veins, arteries, and cell membranes, as well as intricate liquid electronics. Beyond surfactants, nanoparticles have also been shown to aggregate at the interface of immiscible

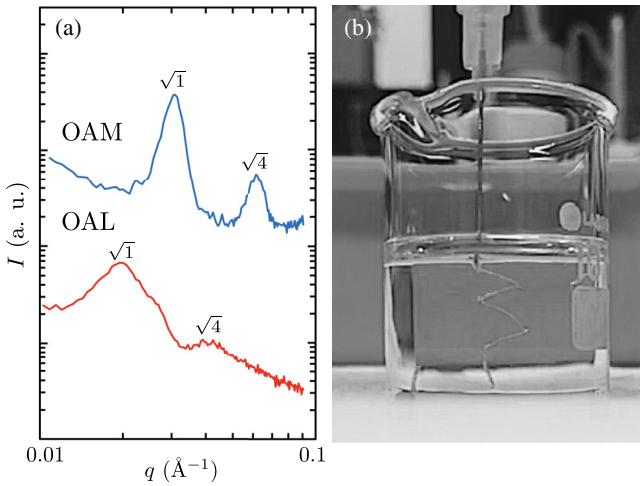

FIG. 4. (a) SAXS patterns for interfacial material formation of 100 mM CPCl solution with OAM (blue) and OAL (red). (b) A self-supporting spiral tube made with manual injection of 425 mM CPCl solution in OA using a 27G needle.

fluids as well and form bicontinuous jammed emulsions (bijels) [16,63,64]. Russell and co-workers have recently introduced a method that takes advantage of nanoparticle jamming at an interface to print desired structures [65,66]. In the work described here, instead of utilizing nanoparticle-polymer or nanoparticle-surfactant jamming, we are able to use self-assembled surfactant-cosurfactant association to create well-defined ordered nanostructures with tunable domain spacing.

In conclusion, our experiments probe the interfacial material formation in an aqueous-oil system, which causes changes in the interfacial instabilities and is dependent on the concentration of the CPCl solution. The interfacial material exhibits typical elastic behavior and is characterized as having a lamellar nanostructure with a domain spacing of approximately 20 nm. Our studies reveal that the micelle-to-lamellar structural transition is due to a cosurfactancy effect in which the CPCl molecules are diluted by the OA molecules, which in turn leads to the formation of an interfacial material exhibiting a lamellar morphology that is able to stabilize immiscible liquid-liquid interfaces. The surfactant concentration can be used as a convenient parameter in such systems to stabilize highly nonequilibrium shapes such as self-supporting structures in liquid-liquid environments. The diversity of possible stable morphologies can lead to new routes in fluids separation and encapsulation in drug delivery, bioprinting, and processing applications.

All of the SAXS measurements were taken at the Materials Characterization Lab (MCL) in the Materials Research Institute (MRI) at Penn State University. This work was supported using start-up funds from the Penn State University and University of Missouri-Kansas City.

*Corresponding author.
rjh64@psu.edu

[1] L. W. Lake, R. T. Johns, W. R. Rossen, and G. A. Pope, *Fundamentals of Enhanced Oil Recovery* (Society of Petroleum Engineers, Richardson, TX, 2014).
[2] J. Stokes and J. Telford, J. Non-Newtonian Fluid Mech. **124**, 137 (2004).
[3] G. Eccleston, J. Colloid Interface Sci. **57**, 66 (1976).
[4] R. Rajabalaya, M. N. Musa, N. Kifli, and S. R. David, Drug. Des. Devel. Ther. **11**, 393 (2017).
[5] G. F. Christopher and S. L. Anna, J. Phys. D **40**, R319 (2007).
[6] J. N. Israelachvili, *Intermolecular and Surface Forces* (Academic Press, San Diego, 2011).
[7] R. J. Hickey, T. M. Gillard, M. T. Irwin, D. C. Morse, T. P. Lodge, and F. S. Bates, Macromolecules **49**, 7928 (2016).
[8] R. J. Hickey, T. M. Gillard, M. T. Irwin, T. P. Lodge, and F. S. Bates, Soft Matter **12**, 53 (2016).
[9] B. H. Jones and T. P. Lodge, Polym. J. **44**, 131 (2012).
[10] F. S. Bates, W. W. Maurer, P. M. Lipic, M. A. Hillmyer, K. Almdal, K. Mortensen, G. H. Fredrickson, and T. P. Lodge, Phys. Rev. Lett. **79**, 849 (1997).
[11] Z. Yang, J. Wei, Y. I. Sobolev, and B. A. Grzybowski, Nature (London) **553**, 313 (2018).
[12] C. G. Palivan, R. Goers, A. Najer, X. Zhang, A. Car, and W. Meier, Chem. Soc. Rev. **45**, 377 (2016).
[13] G. P. Sorenson, K. L. Coppage, and M. K. Mahanthappa, J. Am. Chem. Soc. **133**, 14928 (2011).
[14] D. V. Perroni, C. M. Baez-Cotto, G. P. Sorenson, and M. K. Mahanthappa, J. Phys. Chem. Lett. **6**, 993 (2015).
[15] M. Goldberg, R. Langer, and X. Jia, J. Biomater. Sci., Polym. Ed. **18**, 241 (2007).
[16] C. Huang, J. Forth, W. Wang, K. Hong, G. S. Smith, B. A. Helms, and T. P. Russell, Nat. Nanotechnol. **12**, 1060 (2017).
[17] M. Losurdo, A. Suvorova, S. Rubanov, K. Hingerl, and A. S. Brown, Nat. Mater. **15**, 995 (2016).
[18] C. C. Yang and Y.-W. Mai, Mater. Sci. Eng. R **79**, 1 (2014).
[19] L. Kvitek, A. Panáček, J. Soukupova, M. Kolář, R. Večeřová, R. Prucek, M. Holecova, and R. Zbořil, J. Phys. Chem. C **112**, 5825 (2008).
[20] A. B. Subramaniam, M. Abkarian, and H. A. Stone, Nat. Mater. **4**, 553 (2005).
[21] L. M. Walker and D. M. Kuntz, Curr. Opin. Colloid Interface Sci. **12**, 101 (2007).
[22] S. Friberg, L. Mandell, and M. Larsson, J. Colloid Interface Sci. **29**, 155 (1969).
[23] S. Friberg, P. O. Jansson, and E. Cederberg, J. Colloid Interface Sci. **55**, 614 (1976).
[24] S. E. Friberg and C. Solans, Langmuir **2**, 121 (1986).
[25] T. Suzuki, H. Takei, and S. Yamazaki, J. Colloid Interface Sci. **129**, 491 (1989).
[26] K. Shinoda and H. Saito, J. Colloid Interface Sci. **26**, 70 (1968).
[27] Z. Briceño-Ahumada, A. Maldonado, M. Impéror-Clerc, and D. Langevin, Soft Matter **12**, 1459 (2016).
[28] L. Chiappisi, H. Yalcinkaya, V. K. Gopalakrishnan, M. Gradzielski, and T. Zemb, Colloid Polym. Sci. **293**, 3131 (2015).

[29] S. R. Raghavan, G. Fritz, and E. W. Kaler, Langmuir **18**, 3797 (2002).
[30] B. Kronberg, K. Holmberg, and B. Lindman, *Surface Chemistry of Surfactants and Polymers* (John Wiley & Sons, Chichester, West Sussex, 2014).
[31] E. W. Kaler, A. K. Murthy, B. E. Rodriguez, and J. A. Zasadzinski, Science **245**, 1371 (1989).
[32] N. Schelero, R. Miller, and R. von Klitzing, Colloids Surf. A **460**, 158 (2014).
[33] L. R. Arriaga, D. Varade, D. Carriere, W. Drenckhan, and D. Langevin, Langmuir **29**, 3214 (2013).
[34] M. A. Hartmann, R. Weinkamer, T. Zemb, F. D. Fischer, and P. Fratzl, Phys. Rev. Lett. **97**, 018106 (2006).
[35] N. Schelero, H. Lichtenfeld, H. Zastrow, H. Möhwald, M. Dubois, and T. Zemb, Colloids Surf. A **337**, 146 (2009).
[36] N. Schelero, A. Stocco, H. Möhwald, and T. Zemb, Soft Matter **7**, 10694 (2011).
[37] A. L. Fameau and T. Zemb, Adv. Colloid Interface Sci. **207**, 43 (2014).
[38] A. Stocco, D. Carriere, M. Cottat, and D. Langevin, Langmuir **26**, 10663 (2010).
[39] Y. Michina, D. Carrière, C. Mariet, M. Moskura, P. Berthault, L. Belloni, and T. Zemb, Langmuir **25**, 698 (2009).
[40] C. Noirjean, F. Testard, J. Jestin, O. Tache, C. Dejugnat, and D. Carriere, Soft Matter **10**, 5928 (2014).
[41] C. Noirjean, F. Testard, C. Dejugnat, J. Jestin, and D. Carriere, Phys. Chem. Chem. Phys. **18**, 15911 (2016).
[42] A. Song, S. Dong, X. Jia, J. Hao, W. Liu, and T. Liu, Angew. Chem., Int. Ed. Engl. **44**, 4018 (2005).
[43] D. Zhao, H. Li, A. Song, and J. Hao, Chin. Sci. Bull. **54**, 3953 (2009).
[44] H. Li and J. Hao, J. Phys. Chem. B **112**, 10497 (2008).
[45] S. Simon, S. Subramanian, B. Gao, and J. Sjöblom, Ind. Eng. Chem. Res. **54**, 8713 (2015).
[46] J. P. Rane, V. Pauchard, A. Couzis, and S. Banerjee, Langmuir **29**, 4750 (2013).
[47] V. Pauchard, J. P. Rane, and S. Banerjee, Langmuir **30**, 12795 (2014).
[48] Z. Niroobakhsh and A. Belmonte, J. Non-Newtonian Fluid Mech. **261**, 111 (2018).
[49] Z. Niroobakhsh, M. Litman, and A. Belmonte, Phys. Rev. E **96**, 053102 (2017).
[50] J. J. Cardiel, D. Takagi, H. Tsai, and A. Q. Shen, Soft Matter **12**, 8226 (2016).
[51] T. Podgorski, M. C. Sostarecz, S. Zorman, and A. Belmonte, Phys. Rev. E **76**, 016202 (2007).
[52] E. Ambrose, in *Symposia of the Faraday Society* (Royal Society of Chemistry, London, 1971), Vol. 5, pp. 175–186.
[53] J. Ferguson, Journal of the American Oil Chemists' Society **45**, 120 (1968).
[54] C. Das, M. G. Noro, and P. D. Olmsted, Phys. Rev. Lett. **111**, 148101 (2013).
[55] M. Corti, A. Raudino, L. Cantù, J. Theisen, M. Pleines, and T. N. Zemb, Langmuir **34**, 8154 (2018).
[56] M. J. Rosen and J. T. Kunjappu, *Surfactants and Interfacial Phenomena* (John Wiley & Sons, Hoboken, 2012).
[57] See Supplemental Material at http://link.aps.org/supplemental/10.1103/PhysRevLett.122.178003 for detailed description of experimental methods and proof of results in the main text.
[58] J. Bhattacharjee, V. Aswal, P. Hassan, R. Pamu, J. Narayanan, and J. Bellare, Soft Matter **8**, 10130 (2012).
[59] D. Varade, T. Joshi, V. Aswal, P. Goyal, P. Hassan, and P. Bahadur, Colloids Surf. A **259**, 95 (2005).
[60] T. Zemb, M. Dubois, B. Deme, and T. Gulik-Krzywicki, Science **283**, 816 (1999).
[61] B. Jonsson and H. Wennerstroem, J. Phys. Chem. **91**, 338 (1987).
[62] D. F. Evans and H. Wennerstrom, *The Colloidal Domain: Where Physics, Chemistry, Biology, And Technology Meet* (Wiley-Vch, New York, 1999).
[63] M. F. Haase, K. J. Stebe, and D. Lee, Adv. Mater. **27**, 7065 (2015).
[64] C. Huang, M. Cui, Z. Sun, F. Liu, B. A. Helms, and T. P. Russell, Langmuir **33**, 7994 (2017).
[65] A. Toor, S. Lamb, B. A. Helms, and T. P. Russell, ACS Nano **12**, 2365 (2018).
[66] J. Forth, X. Liu, J. Hasnain, A. Toor, K. Miszta, S. Shi, P. L. Geissler, T. Emrick, B. A. Helms, and T. P. Russell, Adv. Mater. **30**, 1707603 (2018).